Path Variation and Image Segmentation

Pablo Andrés Arbeláez and Laurent D. Cohen

CEREMADE, UMR CNRS 7534 Université Paris Dauphine,
Place du maréchal de Lattre de Tassigny,
75775 Paris cedex 16, France
arbelaez@ceremade.dauphine.fr, cohen@ceremade.dauphine.fr

Abstract. We present a method to address low-level segmentation of monochrome images. The problem is formulated in the framework of energy minimizing paths, as the partition induced by an energy and a set of sources. We study an energy of particular interest, called the path variation, whose application preserves the geometric structure of the image. Then, choosing the image extrema as sources, we construct a piecewise constant approximation of the image, designated as the extrema mosaic. Finally, we apply the method as a presegmentation to the Mumford and Shah variational model.

1 Introduction

Image segmentation is a fundamental issue in the field of computer vision. Its complexity may be understood by the fact that partitioning an image domain into "important" regions amounts to make an interpretation of the scene depicted. As pointed out by a recent study [16], the definition and evaluation of human segmentation represents by itself a difficult problem where recognition and subjectivity seem to play an important role. Therefore, the introduction of semantic information appears as a crucial step in the elaboration of any high level computer vision system.

Nevertheless, a first task is the extraction of the information provided by the image data without prior knowledge of its content. The present paper addresses this low level segmentation issue, focusing on monochrome digital images. The proposed approach relies on the formulation of the problem in the framework of energy minimizing paths, where an energy is defined as the surface of minimal action of a potential function. Then, a partition of the image domain can be obtained by considering the influence zones of a set of source points. Therefore, in this context, the problem is transferred to the definition of the energy and the selection of the sources.

The concept of *variation* or *total variation* of a real valued one dimensional function was introduced by Jordan [9] as early as in 1881. This functional has found application in various branches of mathematics [15, 19], particularly, in the definition of the Stieltjes integral. In the regular framework, the variation of a function $f : [0, L] \to \mathbb{R}$ can be written as [8]:

$$v(f) = \int_0^L |f'(s)|\, ds \ . \tag{1}$$

Several definitions of the variation exist for functions of multiple variables. If $u : \Omega \subset \mathbb{R}^2 \to \mathbb{R}$ is a continuously differentiable function, the most straightforward generalization consists in replacing the derivative in (1) by the gradient:

$$V(u) = \int_{\Omega} \|\nabla u(x)\| \, dx \quad . \tag{2}$$

In the context of image analysis, the general version of (2), allowing discontinuities in the function, was first used by Osher and Rudin [20]. Since then, the space of functions of bounded variation $BV(\Omega)$ has been used to model images and total variation minimization has been successfully applied to image restoration and denoising problems [23, 22, 2, 6].

In this paper, we study a notion of variation for two variable functions based on energy minimizing paths. Precisely, we define the *path variation* as the minimal total variation of the function on all the paths that join two points of the domain. Furthermore, we propose a discrete interpretation of the path variation and discuss its application as a low-level image segmentation method.

The rest of the paper is organized as follows. The basic concepts of the minimal paths approach are described in Sect. 2. The path variation is presented in Sect. 3. In Sect. 4, we study the partitions of the image domain induced by the path variation and use a scale-space representation of the image to select a set of sources. Finally, in Sect. 5, we present an example of the application of our approach as a preprocessing step to improve mid level variational methods for segmentation.

2 Definitions

This introductory section presents the general framework for the rest of the paper. Basic definitions are recalled and the notations settled.

2.1 Minimal Paths

Let $\Omega \subset \mathbb{R}^2$ be a compact connected domain in the plane and $x, y \in \Omega$ two points. A *path* from x to y designates an injective $\mathcal{C}^1$ function $\gamma : [0, L] \to \Omega$ such that $\gamma(0) = x$ and $\gamma(L) = y$. The image of γ is then a rectifiable simple curve in the domain. The path is parameterized by the arclength parameter s, i.e: $\|\dot{\gamma}(s)\| = 1$, $\forall s \in [0, L]$ and L represents the Euclidean length of the path. The set of paths from x to y is noted by Γ_{xy}.

Definition 1. *The* ***surface of minimal action****, or* ***energy****, of a potential function $P : \Omega \times \mathcal{S}^1 \to \mathbb{R}^+$, with respect to a source point $x_0 \in \Omega$, evaluated at x, is defined as*

$$E_0(x) = \inf_{\gamma \in \Gamma_{x_0 x}} \int_0^L P(\gamma(s), \dot{\gamma}(s)) \, ds \quad .$$

When P depends only on the position $\gamma(\cdot)$ and is strictly positive, the field of geometrical optics provides the following physical interpretation of the energy: the potential $P : \Omega \to \mathbb{R}^+$ represents a refractive field of indices of an optical medium and E_0, called the *eikonal* in this context, supplies the optical length of the light rays. Then, the relation between the energy and the potential can be expressed by the *Eikonal Equation*:

$$\|\nabla E_0(x)\| = P(x) \ , \tag{3}$$

with boundary condition $E_0(x_0) = 0$.
In this particular case, the computation of the energy can be performed using Sethian's *Fast Marching* method [24, 4]. Noticing that the information is propagating outwards from the sources, the Fast Marching uses an up-wind scheme to construct a correct approximation of the viscosity solution of (3).

Energy minimizing paths have been used to address several problems in the field of computer vision, where the potential is generally defined as a function of the image. Examples include the global minimum for active contour models [4], shape from shading [10], continuous scale morphology [11], virtual endoscopy [5] and perceptual grouping [3].

2.2 Energy Partitions

The energy with respect to a set of sources $S = \{x_i\}_{i \in J}$ is defined as the minimal individual energy:

$$E_S(x) = \inf_{i \in J} E_i(x) \ .$$

In the presence of multiple sources, a valuable information is provided by the interaction in the domain of a source x_i with the other elements of S, which is expressed through its *influence zone*:

$$Z_i = \{x \in \Omega | \, E_i(x) < \ E_j(x), \forall j \in J, \, j \neq i\} \ .$$

Thus, the influence zone, or briefly the *zone*, is a connected subset of the domain, completely determined by the energy and the rest of the sources. Their union is noted by:

$$Z(E, S) = \bigcup_{i \in J} Z_i \ .$$

The *medial set* is defined as the complementary set of $Z(E, S)$:

$$M(E, S) = \{x \in \Omega \, | \, \exists \, i, j \in J, \, i \neq j : \, E_S(x) = E_i(x) = E_j(x)\} \ .$$

Definition 2. *The* ***energy partition*** *of a domain Ω with respect to an energy E and a set of sources S, is defined as:*

$$\Pi(E, S) = Z(E, S) \bigcup M(E, S) \ .$$

As a first example, if the potential is constant, e.g. $P \equiv 1$, then the energy at x,

$$G_0(x) = \inf_{\gamma \in \Gamma_{x_0 x}} \int_0^L ds \ ,$$

becomes the geodesic distance to the source, or the Euclidean length of the shortest path between x_0 and x. Moreover, if the domain is convex, then G_0 coincides with the Euclidean distance to x_0. If a set of sources $S = \{x_i\}_{i \in J}$ is considered, then the medial set $M(G, S)$ corresponds to the Voronoi diagram and the zones $Z(G, S)$ to the Voronoi cells.

2.3 Mosaic Images

Therefore, in this context, the image segmentation problem is transferred to the definition of an energy from the image data and the selection of a set of sources. Nevertheless, in practice, digital images are subsampled on the discrete grid. Consequently, important parts of the medial set often fall in the intergrid space. For region based segmentation purposes, an alternative to surround this problem is to consider an energy partition composed only by zones. Thus, the elements of the medial set that would fall exactly in the grid are assigned to one of their neighboring influence zones.

Then, an approximation of the image can be constructed by the assignation of a *model* to represent each influence zone. The model is determined by the distribution of the image values on the zone; simple models are the mean or median value on the influence zone and source's level. When the model is constant, the valuation of each zone by its model produces a piecewise constant approximation of the image, referred in the sequel as a *mosaic image*.

3 The Path Variation

In the usual approach for the application of minimal paths to image analysis, a large part of the problem consists in the design of a relevant potential for a specific situation and type of images. However, we adopt a different perspective and use the notions of the previous section for the study of a particular energy, whose definition depends only on geometric properties of the image.

3.1 Continuous Domain

For functions of one real variable, the variation is a functional with known properties [8, 19]. It was introduced by Jordan [9] as follows:
Let $f : [0, L] \to \mathbb{R}$ be a function, $\sigma = \{s_0, ..., s_n\}$ a finite partition of $[0, L]$ such that $0 = s_0 < s_1 < ... < s_n = L$ and Φ the set of such partitions.
The *total variation* of f is defined as

$$v(f) = \sup_{\sigma \in \Phi} \sum_{i=1}^{n} |f(s_i) - f(s_{i-1})| \ .$$

Thus, we propose to generalize this notion for two variable functions, by considering the minimal total variation on all the paths that join two points:

Definition 3. *The **path variation** of a function $u : \Omega \subset \mathbb{R}^2 \to \mathbb{R}$ with respect to a source point $x_0 \in \Omega$, evaluated at x, is defined as*

$$V_0(u)(x) = \inf_{\gamma \in \Gamma_{x_0 x}} v(u \circ \gamma) \ .$$

Definition 4. *The space of functions of **bounded path variation** of Ω, noted by $BLV(\Omega)$ is defined by*

$$BLV(\Omega) = \{u : \Omega \to \mathbb{R} \mid \forall x_0, x \in \Omega,\ \exists\, \hat{\gamma} \in \Gamma_{x_0 x} \ :\ V_0(u)(x) = v(u \circ \hat{\gamma}) < \infty\} \ .$$

In the sequel, we suppose that u has bounded path variation. Note that, if $u \in BLV(\Omega)$, then the path variation of u between any couple of points is not only required to be finite but also to be realized by a path. Hence, Def. 4 supposes the existence of geodesics for V. This assumption seems reasonable for digital images; however, it should be noted that geodesics of V are generally not unique:

A path $\gamma \in \Gamma_{xy}$ is said to be *monotone* for u if $u \circ \gamma$ is a monotone function. By definition, if γ is monotone for u, then it is a geodesic for $V(u)$. Conversely, every geodesic for $V(u)$ is a concatenation of monotone paths.

In the regular framework, the path variation can be characterized as an energy, in the sense of Def. 1 :

Proposition 1. *If $u \in \mathcal{C}^1(\Omega) \bigcap BLV(\Omega)$, then the path variation $V_0(u)$ is the surface of minimal action of the potential $P = |D_{\dot{\gamma}} u|$, the absolute value of the directional derivative of u in the tangent direction of the path.*

Proof. If $f \in \mathcal{C}^1([0, L])$, then the total variation can be expressed in terms of its derivative [8] by the formula:

$$v(f) = \int_0^L |f'(s)|\, ds \ .$$

Thus, if u is a continuously differentiable function, then Def 3. can be reformulated as:

$$V_0(u)(x) = \inf_{\gamma \in \Gamma_{x_0 x}} \int_0^L |\frac{\partial (u \circ \gamma)}{\partial s}(s)|\, ds \ .$$

Hence, we obtain the following expression for the path variation:

$$V_0(u)(x) = \inf_{\gamma \in \Gamma_{x_0 x}} \int_0^L |D_{\dot{\gamma}} u(\gamma(s))|\, ds \ .$$

□

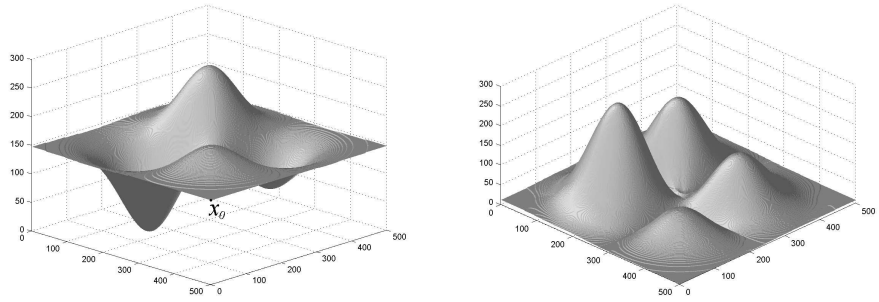

Fig. 1. Simple example: graphs of u and $V_0(u)$.

The intuitive interpretation of the path variation is illustrated in Fig. 1: consider a particle moving along the graph of the function depicted on the left and starting at the source x_0. Then, as shown on the right, the value of $V_0(u)$ evaluated at x represents the minimal sum of ascents and descents to be travelled to reach the point x.

The path variation expresses the same notion as the concept of *linear variation*, introduced in [13], though in a formulation without paths, as a part of a geometric theory for functions of two variables .

The *component* of u containing x, noted by K_x, designates the maximal connected subset of Ω such that $u(y) = u(x),\ \forall y \in K_x$. The level of a component K is noted by $u(K)$ and the set of components of u is noted by T_u. The components of a continuous function are closed and pairwise disjoint subsets of Ω. For continuously differentiable functions, the components of the nonsingular levels (i.e., levels t such that $0 \notin \nabla u(u^{-1}(t))$) coincide with the level lines of u and can be described as Jordan curves.

The importance of the components for the path variation is expressed by the following proposition, whose proof is an immediate consequence of Def. 3.

Proposition 2. *The path variation acts on the component space T_u:*

$$\forall\, x, y \in \Omega,\ K_x = K_y \Rightarrow \forall\, x_0,\, V_0(u)(x) = V_0(u)(y)\ .$$

Therefore, each component of $V_0(u)$ is a union of components of u. Furthermore, for a set of sources S, each element of $\Pi(V(u), S)$ is a union of components of the function. Thus, since the energy partitions induced by the path variation preserve this geometric structure of the function, $V(u)$ presents a particular interest for image analysis. Moreover, the energy partitions induced by the path variation are invariant under linear contrast changes.

Figure 2 illustrates the application of the path variation on a test function. The set of sources in this case is $S = \{x_0, x_1\}$, where x_0 is the upper left and

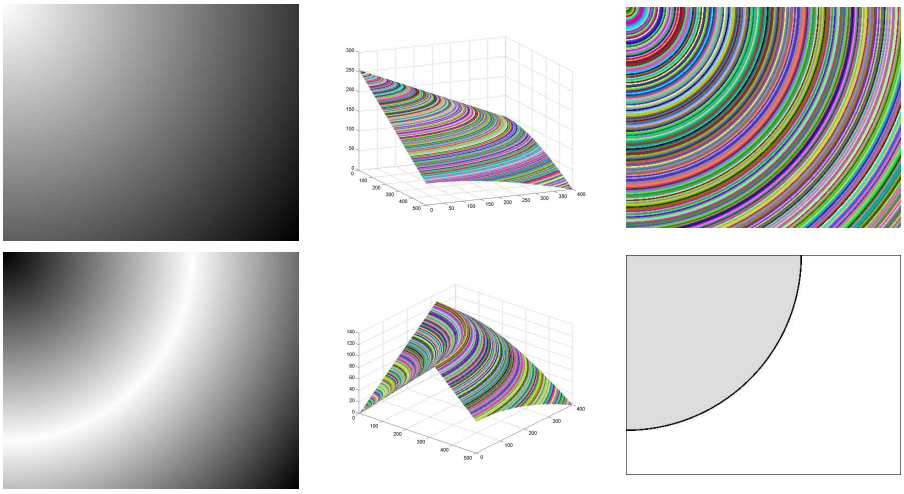

Fig. 2. Top: u its graph and its components in RLUT. Bottom: $V_S(u)$, its graph and energy partition.

x_1 the lower right corners of the domain and the function is given by the simple formula $u(x) = c\|x - x_0\|$. The top row shows u, its graph and its components in random lookup table (RLUT). The bottom row displays the intensity image of $V_S(u)$, its graph and the energy partition $\Pi(V(u), S)$. Notice how the path variation preserves the component structure of u and modifies only their level. The medial set $M(V(u), S)$, shown in black, corresponds in this case to the component whose level is the average of the sources' levels.

3.2 Discrete Domain

In this paragraph, we propose a discrete interpretation for the path variation. Thus, we consider that the image u has been sampled on a uniform grid. A first remark is that, since the potential of the path variation in Prop. 1 depends not only on the position but also on the path direction, the Fast Marching method cannot be used for its construction.

Nevertheless, in a discrete domain, the component structure of a function can be represented by an adjacency graph G, where the nodes correspond to discrete components and the links join neighboring components. Thus, G is the equivalent of T_u in the discrete space. Since V acts on the components of the function, we propose to construct the discrete path variation directly on G.

A path on G joining the components of two points p and q is a set $\gamma = \{K_0, ..., K_n\}$ such that $K_p = K_0$, $K_n = K_q$, K_i and K_{i-1} are neighbors, $\forall i = 1, ..., n$. The set of such paths is noted by Γ_{pq}^G. Each element of Γ_{pq}^G corresponds then to a class of discrete paths between p and q.

Fig. 3. Manual sources and corresponding mosaic image.

Thus, the expression of the discrete path variation of u at a point q with respect to the source p becomes

$$V_p(u)(q) = \min_{\gamma \in \Gamma_{pq}^G} \sum_{i=1}^{n} |u(K_i) - u(K_{i-1})| \ .$$

Hence, the calculation of $V_p(u)$ is reduced to finding the path of minimal cost on a graph. This classical problem can be solved using a greedy algorithm [7, 14]. The complexity of this implementation for the path variation is then $O(Nlog(N))$, where N is the total number of discrete components of the image. Furthermore, if u takes integer values, the sorting step in the update of the narrow band can be suppressed and the complexity is reduced to $O(N)$.

4 Sources Selection

In this section, we intend to apply the energy partitions induced by the path variation to image analysis. For this purpose, once the energy has been defined, the second step is the selection of a set of sources.

In order to use a surface of minimal action to address image segmentation problems, the choice of the sources is a critical issue. Indeed, since Def. 1 is based on an integration along the paths, the partitions defined by this type of energies are very sensitive to the location of the sources. Furthermore, replacing a source $x_i \in S$ by another point $x_i' \in Z_i$ usually modifies the corresponding energy partition.

Therefore, the set of sources should be physically representative of the image content. Ideally, for region based segmentation purposes, each zone should correspond to a significant feature in the image and their boundaries should describe

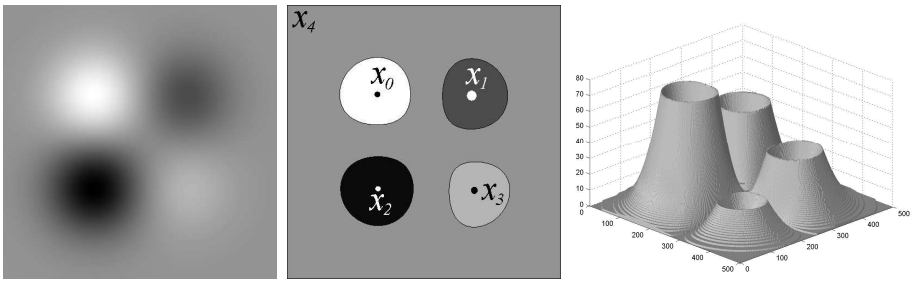

Fig. 4. From left to right: original image, mosaic image with sources and graph of the energy.

the contours of the objects. Figure 3 shows the mosaic corresponding to the energy partition $\Pi(V(u), S)$, where a set S composed by 25 sources was placed by hand. The intended goal was to provide a general description of the scene represented in the image, but also to include perceptually important details as the eye or the building on the background.

4.1 The Extrema Partition

Figure 4 exemplifies the problem of sources selection on the smooth image of the left. An acceptable segmentation of this "scene" should be composed by four approximately circular regions on a gray background. A natural solution would be to take the extrema of the four peaks as sources for the "features" and the border of the domain as the source representing the background. The image on the middle shows this choice of sources and the mosaic corresponding to the energy partition $\Pi(V(u), S)$, where the source intensity was taken as zone model. On the right, we can observe the graph of the energy $V_S(u)$.

Therefore, in the regular framework, the image extrema appear as natural candidates for the sources. The energy partition induced by the path variation and the set of extremal components, $\Pi(V(u), ext(u))$, will be called the *extrema partition* of the image u and the corresponding mosaic image the *extrema mosaic*.

In real images, the choice of the path variation as the energy and the spatial distribution of the intensity extrema provide a compromise between content conservation and simplification in the extrema mosaic. Perceptually, the effects of this piecewise constant approximation of the image can be better appreciated when the ratio between the number of components in the original image and the number of zones is high. Figure 5 shows an example where this ratio is 68. On the left, we can observe the original image and, on the right, its extrema mosaic. This image illustrates three properties of the extrema partition. First, a contrast enhancement in the butterfly's wings. Second, a reduction of the blur in the background, caused by the absorption of blurred contours and transition components by neighboring zones. Finally, note how the boundaries of the zones model accurately the contour information and, particularly, semantically important characteristics of edges such as corners and junctions.

Fig. 5. Row 1: original image and extrema mosaic.

4.2 Anisotropic Diffusion

The extrema mosaic can be seen as a decomposition of the image in elemental zones or as a first abstraction to the image data. Nevertheless, the presence of textures and noise in natural images produces a large number of extrema in the image intensity. Consequently, the extrema partition is often composed by a large number of small zones. The question is then how to reduce the number of extrema while preserving the image structure. In this paragraph, we propose to address the issue using a scale-space representation of the image.

Therefore, we consider the regularized version [1, 25] of the classical approach proposed by Perona and Malik [21]. In this method, a filtered image $u_t = u(x,t)$ is constructed as a solution of the nonlinear diffusion equation:

$$\frac{\partial u}{\partial t} = \mathrm{div}(g(|\nabla(G_\sigma * u)|^2)\nabla u) \ , \tag{4}$$

where G_σ denotes a Gaussian kernel of variance σ and $g(\cdot)$ is a positive *diffusivity function*. Reflecting boundary conditions are considered and the initial state $u_0 = u(x,0)$ coincides with the original image.

For the results presented in this paper, we used the diffusivity :

$$g(s) = \begin{cases} 1, \text{ if } s \leq 0 \\ 1 - exp\left(\frac{-3.315}{(s/\kappa)^4}\right), \text{ if } s > 0 \end{cases}$$

where κ is the contrast parameter that regulates the selective smoothing process. This diffusivity was reported in [27] to lead to better results than the original functions in [21].

The main characteristic of anisotropic diffusion is the fact that intraregional smoothing is preferred to interregional smoothing. Thus, homogeneous regions

are smoothed in the filtered image u_t, while the edge information is enhanced. Therefore, the number of extrema in the filtered image, noted by $ext(u_t)$, decreases rapidly when the scale is augmented. These properties make of $ext(u_t)$ an interesting candidate for the set of sources of the energy partition. Two choices are then possible, either consider the extrema partition of the filtered image, $\Pi(V(u_t), ext(u_t))$, or go back to the initial image u_0 and construct the partition $\Pi(V(u_0), ext(u_t))$.

Figure 6 illustrates this method for the selection of sources. The initial image u_0 was the extrema mosaic of the *cameraman*, shown on top-left. The parameters of the anisotropic diffusion filtering were $\sigma = 1$ and $\kappa = 30$. The filtered image u_t is shown on top-right, for the scale $t = 180$. The number of extremal components was 8412 in the original image and 261 in the smoothed image. Middle-left shows the extrema mosaic of u_t and middle-right displays the mosaic of $\Pi(V(u_0), ext(u_t))$. It can be observed how both energy partitions preserve the image structure, in spite of the reduction in the number of sources. The main difference lies in the regularization of the zones in the filtered image with respect to the zones obtained with the initial image, as can be seen in the bottom row, where the two partitions are shown.

Hence, the use of anisotropic diffusion is helpful for the selection of sources, however, an excessive filtering would destroy the contour information and this method requires a post processing step.

Conversely, our approach allows to construct an partition with a small number of regions, starting from an image filtered by anisotropic diffusion. This idea was used in [26] to reduce the oversegmentation produced by the watershed transform.

5 Path Variation and Variational Models

The presented approach uses only low level information for the construction of a partition. However, the introduction of higher level cues is often required for the segmentation process. In this section, we combine our method with the Mumford and Shah model.

Variational methods have been widely used to address image segmentation problems. In these approaches, the expectations about the objects in the image are expressed through a functional. A popular example is the model proposed by Mumford and Shah [18]. In its general version, a segmentation of the image u corresponds to a piecewise smooth function f that minimizes the functional:

$$J(f, B) = \int_{\Omega} (f - u)^2 dx + \mu \int_{\Omega \setminus B} \|\nabla f\|^2 dx + \mathcal{H}^1(B) \ , \tag{5}$$

where B is the set of boundaries and $\mathcal{H}^1$ is the one dimensional Hausdorff measure. The usual interpretation of this functional is the following: the first is a data fidelity term, the second controls the regularity of the approximation outside the boundaries and the third penalizes their length. Finally, the scale μ

weights the balance between the terms. Hence, in this approach, the objects of the scene are modelled as homogeneous regions with short boundaries.

The virtues of the Mumford and Shah functional are widely recognized [17]. Figure 7 presents an experiment to illustrate the relevance in the use of the extrema mosaic as a preliminary step for a variational approach to segmentation. We considered the piecewise constant version of the Mumford and Shah functional [12], with the final scale determined by the number of regions N. The method was applied to the *cameraman* test image and its extrema mosaic. The graph of Fig. 7 depicts the PSNR between the two cartoon like segmentations and the original image, when N ranges from 1 to 1000. The dash line corresponds to the original image and the solid line to its EM. It can be observed how, when the required final number of regions is small ($N < 450$), the application of the EM increases the quality of the segmentation. Figure 7 shows, on the first row, the segmentations for $N = 25$, where the PSNR is increased by 3,61 dB. Notice how, in spite of the low number of regions, the EM permits the detection of perceptually important details such as the face of the cameraman or his silhouette. When, $N \geq 450$ the result with both initial images is very similar, as shown in the second row of Fig. 7, where $N = 800$.

6 Conclusion and Perspectives

It should be noted that the use of the path variation for image segmentation assumes a certain homogeneity in the definition of feature. The method presented for the selection of the sources can be improved, considering the results obtained with hand placed sources. We presented a method for low level segmentation, using only geometric information of the image. The approach provides a piecewise constant approximation of the image that models accurately the contour information. The extrema mosaic can be used as a preprocessing step for mid and high level segmentation methods.

Finally, this paper focused on monochrome images in order to emphasize the mathematical formulation and properties of the path variation. However, the results presented can be applied to color images directly by considering the brightness component. The generalization of our approach to color images will be the subject of our next report.

Acknowledgments

The authors wish to thank the blind reviewers, whose comments and suggestions contributed to improve this paper.

References

1. F. Catté, P. L. Lions, J. M. Morel, and T. Coll. Image selective smoothing and edge detection by nonlinear diffusion. *SIAM J. Numer. Anal.*, 29(1):182–193, 1992.

2. A. Chambolle and P.L. Lions. Image recovery via total variation minimization and related problems. *Numerische Mathematik*, 76:167–188, 1997.
3. L. D. Cohen. Multiple contour finding and perceptual grouping using minimal paths. *Journal of Mathematical Imaging and Vision*, 14(3):225–236, 2001.
4. L. D. Cohen and R. Kimmel. Global minimum for active contour models: A minimal path approach. *International Journal of Computer Vision*, 24(1):57–78, August 1997.
5. T. Deschamps and L. D. Cohen. Fast extraction of minimal paths in 3d images and applications to virtual endoscopy. *Medical Image Analysis*, 5(4):281–299, 2001.
6. F. Dibos and G. Koepfler. Global total variation minimization. *SIAM Journal of Numerical Analysis*, 37(2):646–664, 2000.
7. E. W. Dijkstra. A note on two problems in connection with graphs. *Numerische Mathemetic*, 1:269–271, 1959.
8. E. Hewitt and K. Stromberg. *Real and Abstract Analysis*. Springer Verlag, 1969.
9. C. Jordan. Sur la série de fourier. *C. R. Acad. Sci. Paris Sér. I Math.*, 92(5):228–230, 1881.
10. R. Kimmel and A. M. Bruckstein. Global shape from shading. *CVIU*, 62(3):360–369, 1995.
11. R. Kimmel, N. Kiryati, and A. M. Bruckstein. Distance maps and weighted distance transforms. *Journal of Mathematical Imaging and Vision*, 6:223–233, May 1996. Special Issue on Topology and Geometry in Computer Vision.
12. G. Koepfler, C. Lopez, and J. M. Morel. A multiscale algorithm for image segmentation by variational method. *SIAM Journal on Numerical Analysis*, 31(1):282–299, 1994.
13. A. S. Kronrod. On functions of two variables. *Uspehi Mathematical Sciences*, 5(35), 1950. In Russian.
14. R. Kruse and A. Ryba. *Data structures and program design in C++*. Prentice Hall, New York, 1999.
15. H. Lebesgue. *Leçons sur l'Intégration et la Recherche des Fonctions Primitives*. Gauthier Villars, 1928.
16. D. Martin, C. Fowlkes, D. Tal, and J. Malik. A database of human segmented natural images and its application to evaluating segmentation algorithms and measuring ecological statistics. In *Proc. ICCV'01*, volume II, pages 416–423, Vancouver, Canada, 2001.
17. J. M. Morel and S. Solimini. *Variational Methods in Image Segmentation*. Birkhauser, 1995.
18. D. Mumford and J. Shah. Optimal approximations by piecewise smooth functions and variational problems. *CPAM*, XLII(5), 1988.
19. I. P. Natansson. *Theory of Functions of a Real Variable*. Frederick Ungar Publishing, New York, 1964.
20. S. Osher and L.I. Rudin. Feature-oriented image enhancement using shock filters. *NumAnal*, 27(4):919–940, 1990.
21. P. Perona and J. Malik. Scale-space and edge detection using anisotrppic diffusion. *PAMI*, 12(7):629–639, 1990.
22. L.I. Rudin and S. Osher. Total variation based image restoration with free local constraints. In *Proc. ICIP*, pages 31–35, 1994.
23. L.I. Rudin, S. Osher, and E. Fatemi. Nonlinear total variation based noise removal algorithms. *Physica D*, 60:259–268, 1992.
24. J. A. Sethian. *Level Set Methods and Fast Marching Methods*. Cambridge University Press, Cambridge, UK, 2 edition, 1999.

25. J. Weickert. *Anisotropic Diffusion in Image Processing*. Teubner, 1998.
26. J. Weickert. Efficient image segmentation using partial differential equations and morphology. *Pattern Recognition*, 34(9):1813–1824, 2001.
27. J. Weickert, B.M. ter Haar Romeny, and M.A. Viergever. Efficient and reliable schemes for nonlinear diffusion filtering. *IP*, 7(3):398–410, March 1998.

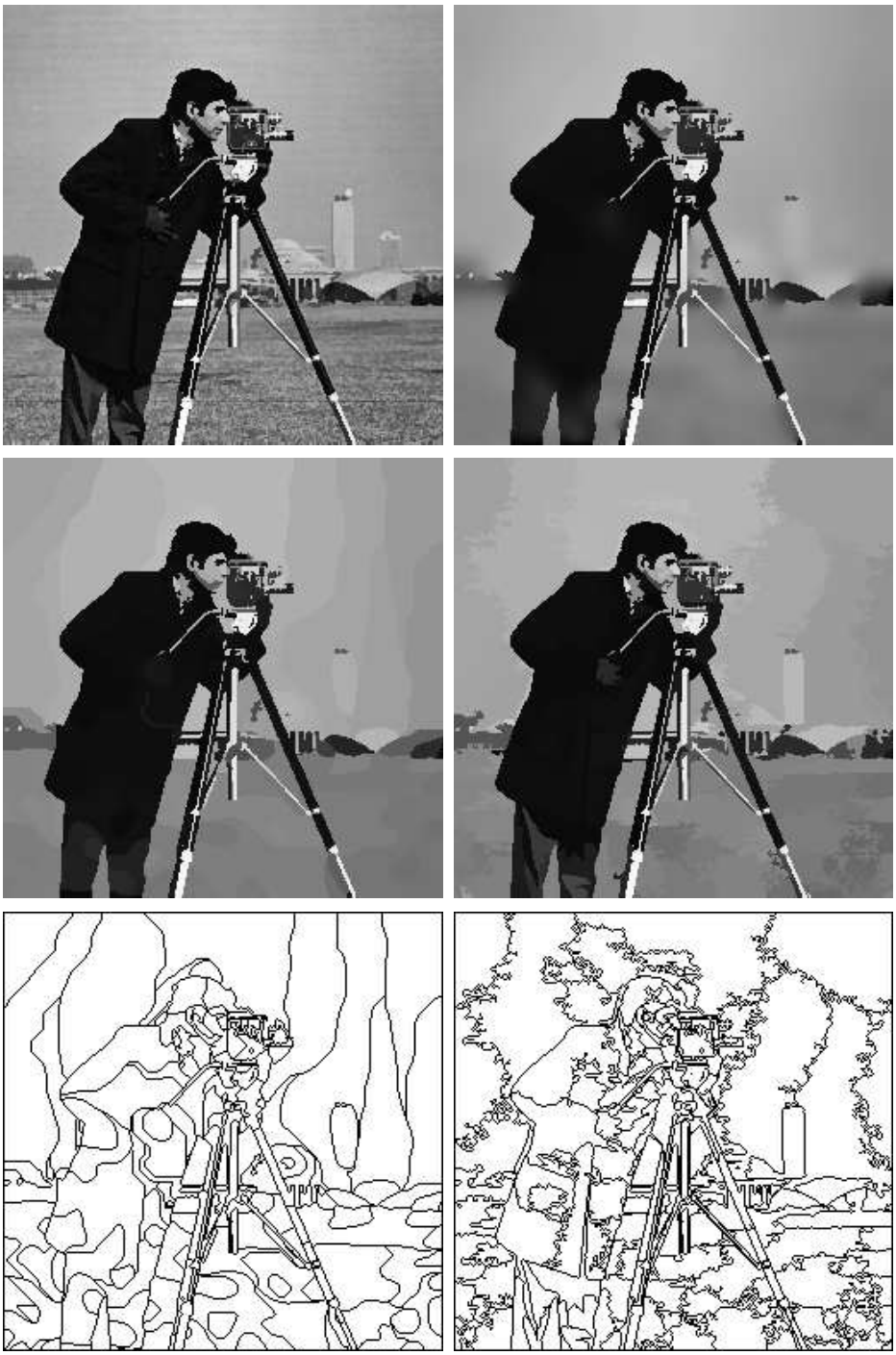

Fig. 6. Sources selection by anisotropic diffusion (see text).

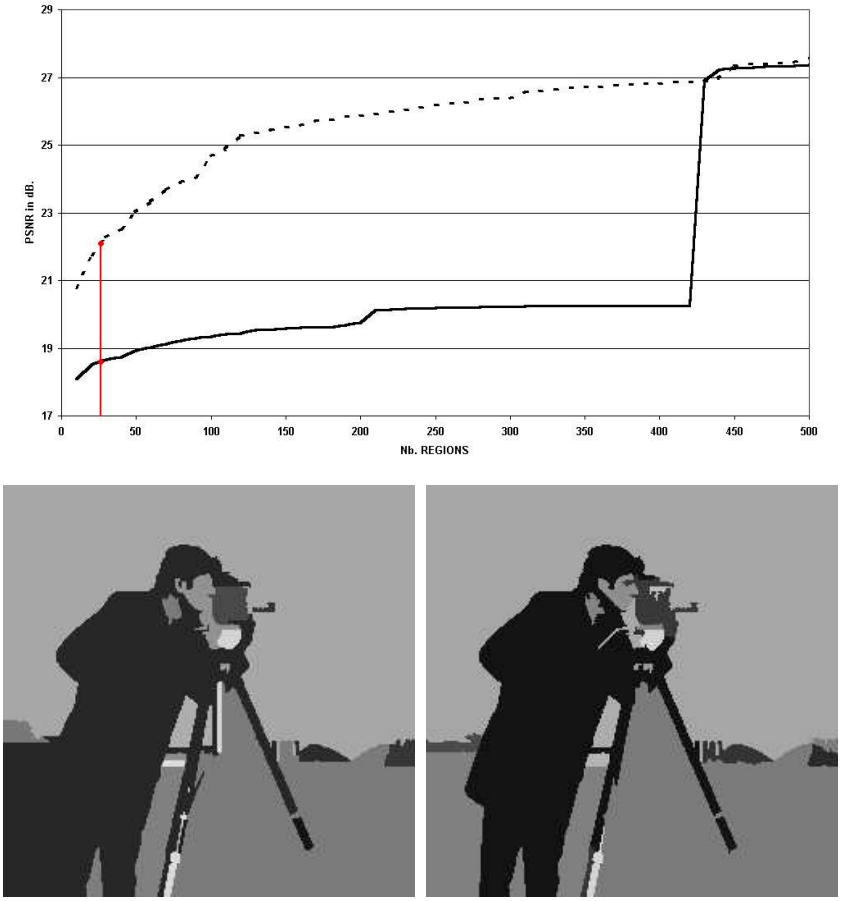

Fig. 7. Extrema Mosaic and Mumford and Shah model (see text).